

Expanding Regulatory T Cells Alleviates Chikungunya Virus-Induced Pathology in Mice

Wendy W. L. Lee,^{a,b} Teck-Hui Teo,^{a,b} Zhisheng Her,^{a*} Fok-Moon Lum,^{a,c} Yiu-Wing Kam,^a Doreen Haase,^a Laurent Rénia,^a Olaf Röttschke,^{a,d,e} Lisa F. P. Ng^{a,c,f}

Singapore Immunology Network, Agency for Science, Technology and Research, Singapore^a; NUS Graduate School for Integrative Sciences and Engineering, National University of Singapore, Singapore^b; Department of Biochemistry, Yong Loo Lin School of Medicine, National University of Singapore, Singapore^c; Department of Microbiology, Yong Loo Lin School of Medicine, National University of Singapore, Singapore^d; School of Biological Sciences, Nanyang Technological University, Singapore^e; Institute of Infection and Global Health, University of Liverpool, Liverpool, United Kingdom^f

ABSTRACT

Chikungunya virus (CHIKV) infection is a reemerging pandemic human arboviral disease. CD4⁺ T cells were previously shown to contribute to joint inflammation in the course of CHIKV infection in mice. The JES6-1 anti-IL-2 antibody selectively expands mouse regulatory T cells (Tregs) by forming a complex with IL-2. In this study, we show that the IL-2 JES6-1-mediated expansion of Tregs ameliorates CHIKV-induced joint pathology. It does so by inhibiting the infiltration of CD4⁺ T cells due to the induction of anergy in CHIKV-specific CD4⁺ effector T cells. These findings suggest that activation of Tregs could also become an alternative approach to control CHIKV-mediated disease.

IMPORTANCE

Chikungunya virus (CHIKV) has reemerged as a pathogen of global significance. Patients infected with CHIKV suffer from incapacitating joint pain that severely affects their daily functioning. Despite the best efforts, treatment is still inadequate. While T cell-mediated immunopathology in CHIKV infections has been reported, the role of regulatory T cells (Tregs) has not been explored. The JES6-1 anti-interleukin 2 (IL-2) antibody has been demonstrated to selectively expand mouse Tregs by forming a complex with IL-2. We reveal here that IL-2 JES6-1-mediated expansion of Tregs ameliorates CHIKV-induced joint pathology in mice by neutralizing virus-specific CD4⁺ effector T (Teff) cells. We show that this treatment abrogates the infiltration of pathogenic CD4⁺ T cells through induction of anergy in CHIKV-specific CD4⁺ Teff cells. This is the first evidence where the role of Tregs is demonstrated in CHIKV pathogenesis, and its expansion could control virus-mediated immunopathology.

Chikungunya virus (CHIKV) is a positive-strand RNA virus belonging to the genus *Alphavirus* (1, 2). Transmitted by the *Aedes* mosquito, its reemergence in 2006 caused major concerns globally (3–5). While chikungunya fever (CHIKF) outbreaks were previously restricted to tropical regions, the range of CHIKV has since expanded to temperate countries such as Italy (6) and France (7). More recently, outbreaks of CHIKF have been reported in the Caribbean islands (8, 9). Since the first autochthonous case reported in December 2013, a total of 1,155,354 cases have been recorded as of 30 January 2015 (8–10), with more than 300 imported cases in the United States (11). The hallmark feature in CHIKF patients is incapacitating arthralgia affecting multiple joints during the acute phase of disease (12). However, it is not uncommon for CHIKF patients to experience persistent joint pain that can last up to several months or years after the initial infection (13, 14). Previous studies have suggested that the pathogenesis of CHIKF is an immediate result of excessive immune attacks (13, 15). Although reports have shown the involvement of T cells in CHIKV immunopathology (16–20), the fine mechanism remains undefined.

Regulatory T cells (Tregs) are a distinct subset of CD4⁺ T cells that prevent exacerbated proinflammatory responses (21, 22) by maintaining tolerance and restoring immune homeostasis during an inflammatory response (23). In various infection models, Tregs have been reported to dampen excessive immune responses triggered by pathogens and minimize damage to the host (24–26). Therefore, elucidating the intriguing role of Tregs would no doubt allow a further understanding of CHIKV immunopathogenesis.

Studies in the CHIKV adult mouse model (27) have shown that CD4^{-/-} mice experienced a reduced CHIKV-induced joint pathology, despite no differences in viremia throughout the course of disease (16), demonstrating a role for CD4⁺ effector T (Teff) cells. Since these cells are a prime target for Tregs, it is crucial to further define how these cells could influence the course of disease by inhibiting pathology (16, 23, 28). In this study, we took advantage of the observation that mouse Tregs can be selectively expanded *in vivo* through the use of interleukin 2 (IL-2) in complex with the anti-IL-2 antibody JES6-1 (IL-2 Ab Cx) (29) to demonstrate the importance of Tregs in regulating CHIKV pathogenesis.

Received 22 April 2015 Accepted 13 May 2015

Accepted manuscript posted online 20 May 2015

Citation Lee WWL, Teo T-H, Her Z, Lum F-M, Kam Y-W, Haase D, Rénia L, Röttschke O, Ng LFP. 2015. Expanding regulatory T cells alleviates chikungunya virus-induced pathology in mice. *J Virol* 89:7893–7904. doi:10.1128/JVI.00998-15.

Editor: T. S. Dermody

Address correspondence to Lisa F. P. Ng, lisa_ng@immunol.a-star.edu.sg.

* Present address: Zhisheng Her, Institute of Molecular & Cell Biology, A*STAR, Singapore, Singapore.

Copyright © 2015, Lee et al. This is an open-access article distributed under the terms of the [Creative Commons Attribution-Noncommercial-ShareAlike 3.0 Unported license](https://creativecommons.org/licenses/by-nc-sa/4.0/), which permits unrestricted noncommercial use, distribution, and reproduction in any medium, provided the original author and source are credited.

doi:10.1128/JVI.00998-15

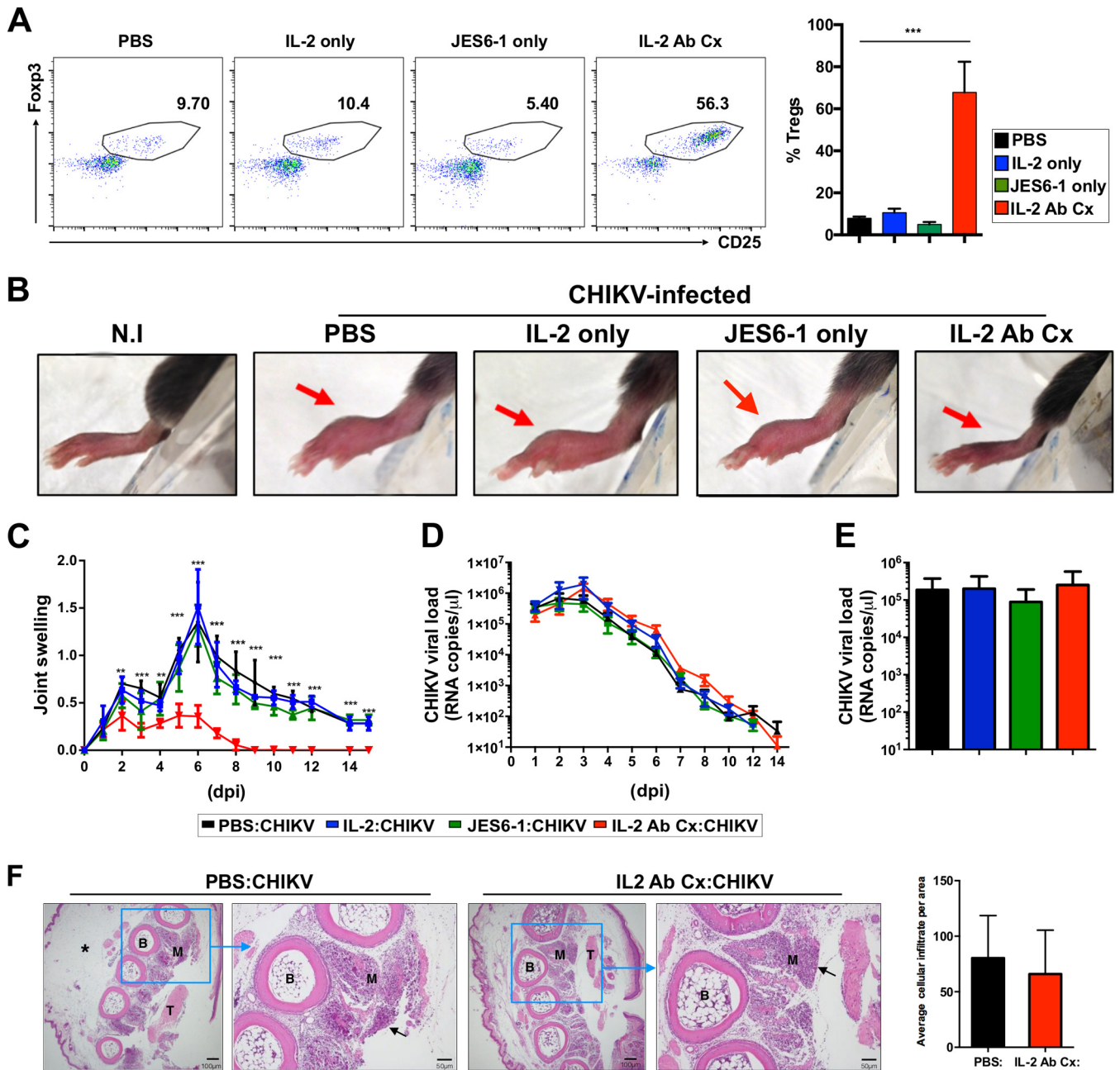


FIG 1 Pretreatment with IL-2 Ab Cx reduces joint swelling in CHIKV-infected mice. WT mice ($n = 5$ per group) were i.p. injected with PBS, IL-2 only, JES6-1 only, or IL-2 Ab Cx daily for 3 days. Blood samples were obtained from tail veins and analyzed with flow cytometry. (A) Representative scatter plots (left) and bar chart of the Foxp3⁺ CD25⁺ peripheral Treg population in mice. Numbers indicate the frequency of Foxp3⁺ CD25⁺ Tregs in total peripheral CD4⁺ cells. Following PBS, IL-2 only, JES6-1 only, or IL-2 Ab Cx treatment, the mice were infected s.c. with 10⁶ PFU CHIKV-SGP011. Noninfected (NI) mice were included as negative control. (B) Representative images showing joint footpad swelling at 6 dpi in CHIKV-infected mice. Red arrows indicate areas of swelling. (C) Joint swelling was measured daily from 1 to 15 dpi. (D) Viremia was determined from blood collected from tail vein from 1 to 14 dpi. (E) Viral load of the infected joint footpad was measured at 6 dpi. All data are means and standard deviations (SD) and are representative of three independent experiments. Statistical analysis was done across all CHIKV-infected groups using one-way ANOVA, followed by Dunnett's posttest comparing each group to the PBS-CHIKV group. (F) Histological analysis of CHIKV-infected footpad samples from 6 dpi pretreated with either PBS or IL-2 Ab Cx and stained with H&E. *, edema; arrows, infiltrates; B, bone; M, muscle; T, tendon. The bar chart shows the average cellular infiltrate per area. Data are means and SD. Statistical analysis was carried out using the Mann-Whitney two-tailed test. **, $P = 0.0017$ (2 dpi joint swelling) or 0.0059 (4 dpi joint swelling); ***, $P < 0.0001$ (3, 5, 7, 8, 9, 10, 11, 12, 14, and 15 dpi joint swelling and IL-2 Ab Cx Treg expansion) or 0.0004 (6 dpi joint swelling).

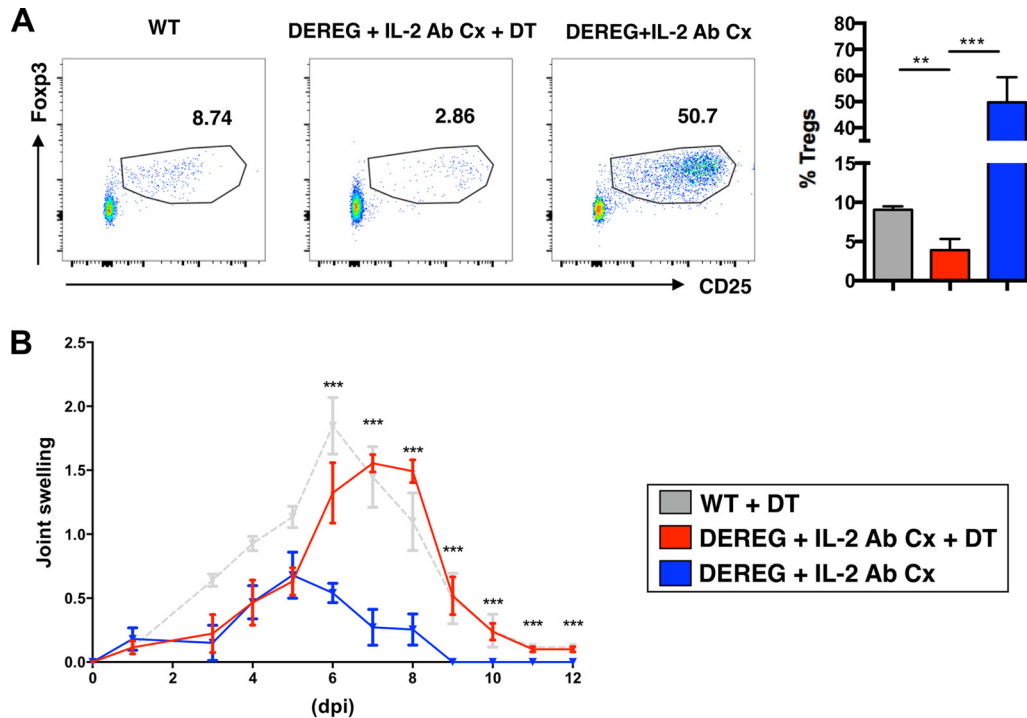


FIG 2 Treg depletion in IL-2 Ab Cx-treated mice results in a loss of protection against CHIKV-induced pathology. WT or DEREK mice ($n = 4$ per group) were treated with IL-2 Ab Cx for 3 days (-5 , -4 , and -3 dpi) followed by DT administration for 2 days to deplete Tregs. Following depletion, mice were infected s.c. with 10^6 PFU CHIKV-SGP011. (A) Representative scatter plot showing peripheral Treg population from DEREK animals with or without IL-2 Ab Cx treatment, followed by DT or no DT treatment. Numbers in scatter plots indicate the Treg population percentage within total $CD4^+$ T cells. Data are means and SD. Statistical analysis was done using one-tailed unpaired t test. **, $P = 0.001$ (WT+DT versus DEREK+IL-2 Ab Cx+DT); ***, $P < 0.0001$ (DEREK+IL-2 Ab Cx+DT versus DEREK+IL-2 Ab Cx). (B) Joint swelling of mice was measured from 0 to 12 dpi following CHIKV infection after IL-2 Ab Cx and DT treatment. Data are means \pm SD. Statistical analysis was done using a two-tailed unpaired t test comparing DEREK+IL-2 Ab Cx+DT and DEREK+IL-2 Ab Cx. ***, $P = 0.0007$ (6 dpi), <0.0001 (7 dpi), <0.0001 (8 dpi), 0.0004 (9 dpi), 0.0003 (10 dpi), <0.0001 (11 dpi), or 0.0001 (12 dpi).

MATERIALS AND METHODS

Study approval. All animals were handled in strict accordance with good animal practice as defined by the National Advisory Committee for Laboratory Animal Research (NACLAR) Guidelines under in facilities licensed by the Agri-Food and Veterinary Authority of Singapore (AVA). Three-week-old C57/BL6J mice were housed in the ABSL3 facility at the Biological Resource Center (BRC) at Biopolis, Singapore. Animals are fed daily and monitored closely by technical officers in charge of the animal facilities. All studies were reviewed and approved by the Institutional Animal Care and Use Committee (IACUC approval no. 120714).

Virus stocks. CHIKV isolate (CHIKV-SGP011) used for *in vitro* and *in vivo* infections in mouse studies was isolated from an outbreak in Singapore in 2008 at the National University Hospital and propagated in C6/36 (30, 31). The titer of SGP011 was determined using standard plaque assays with Vero-E6 cells (30, 31).

Animal studies. Three-week-old wild-type (WT) C57/BL6 female mice were inoculated subcutaneously (s.c.) in the ventral side of the right hind footpad with 10^6 PFU CHIKV in 30 μ l phosphate-buffered saline (PBS). Ten microliters of blood was collected daily from the tail vein for viremia analyses. Footpad joint swelling was determined daily by the measurement of the height and the breadth of the footpad using a caliper and quantified as height times breadth. The degree of inflammation was expressed as the increase relative to the preinfection measurement (day 0), obtained with the following formula: $[(x - \text{day } 0)/\text{day } 0]$, where x is the footpad size measurement for a given day postinfection (dpi) (16, 31–33).

Viremia and viral load measurement. Viral RNA was extracted using a QIAamp viral rRNA minikit (Qiagen) and quantified using QuantiTect probe RT-PCR (Qiagen) with conditions as previously described (16, 31–34). All reactions were performed using a 7900HT Fast real-time

PCR system machine (Applied Biosciences) with thermal cycling conditions as described previously (16, 31–33). The limit of detection is 10 RNA copies/ μ l.

Total RNA isolation and analysis. For total RNA extraction from tissues, mice were anesthetized with ketamine (150 mg/kg)-xylazine (10 mg/kg) and perfused with PBS (33). Joint footpads (the ankle joint and footpad) were obtained and stored in TRIzol (Invitrogen) at -80°C . Tissues were homogenized using a rotor-stator homogenizer (Xiril Dispomix) at 4,000 rpm for 15 s. Homogenized tissues were mixed with 230 μ l of chloroform and centrifuged at 12,000 rpm for 10 min at 4°C . The aqueous phase was collected and isolated for total RNA using an RNeasy minikit (Qiagen) according to the manufacturer's instructions. Quantification of extracted total mRNA was measured by NanoDrop 1000 spectrophotometer (Thermo Scientific). Qualitative real-time PCR (qRT-PCR) was performed using a Kapa SYBR fast one-step qRT-PCR kit (KAPA Biosystems) according to the manufacturer's recommendations in a 10- μ l reaction volume. All reactions were performed using a 7900HT fast real-time PCR system machine (Applied Biosciences). Thermal cycling conditions were as follows: 95°C for 5 min followed by 40 cycles of 95°C for 5 s, 60°C for 30 s, and 95°C for 15 min. The fold change for each gene was calculated relative to the value for noninfected (NI) mice and presented as $2^{-\Delta\Delta\text{CT}}$.

In vivo expansion of Tregs. PBS, 1.5 μ g murine IL-2 (Peprotech), 50 μ g anti-mouse IL-2 (JES6-1) (eBioscience), or 1.5 μ g murine IL-2 complexed with 50 μ g anti-mouse IL-2 were injected intraperitoneally (i.p.) daily for 3 days. Fifteen microliters of blood were collected from the tail vein to check for Treg expansion. Briefly, blood was lysed and fixed using BD fluorescence-activated cell sorting (FACS) lysing buffer (BD Biosciences) and washed twice with PBS. Cells were stained with anti-CD4 (BD

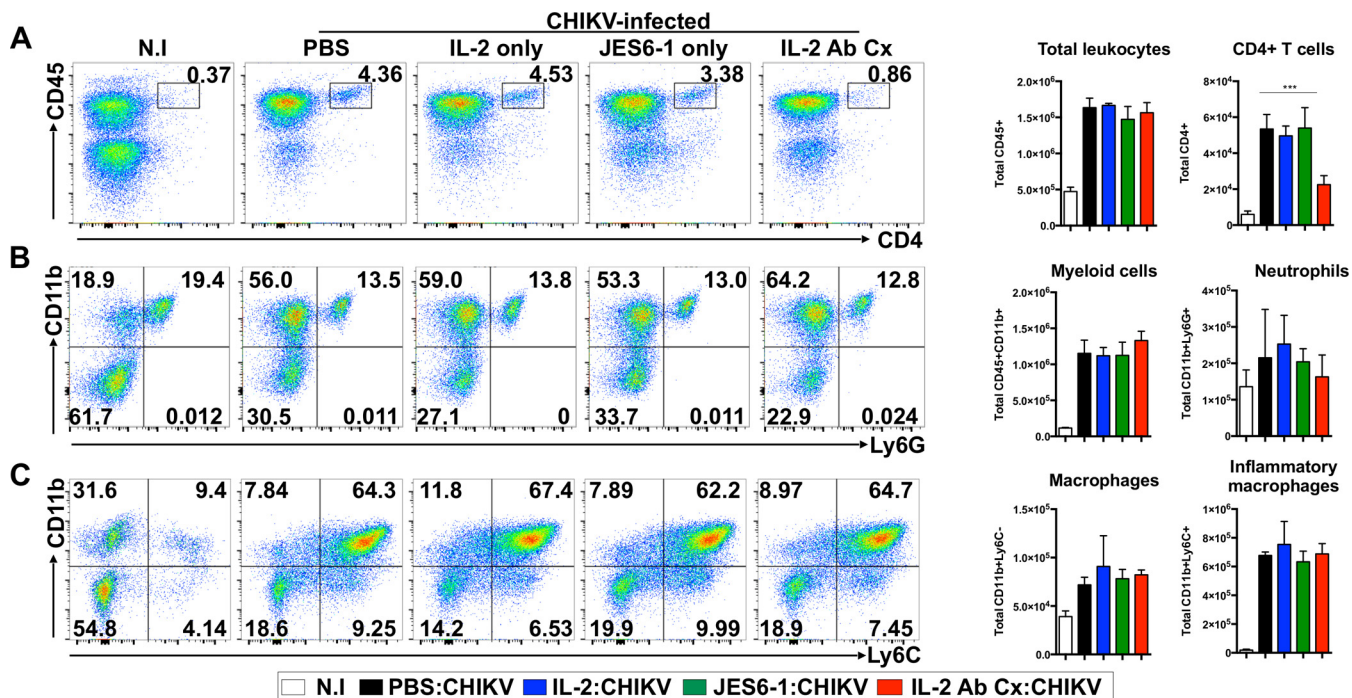


FIG 3 Pretreatment with IL-2 Ab Cx abrogates CD4⁺ infiltration into the joint footpads of CHIKV-infected mice. WT mice ($n = 5$ per group) were infected s.c. with 10^6 PFU CHIKV-SGP011 after treatment with PBS, IL-2 only, JES6-1 only, or IL-2 Ab Cx. Joint footpad cells from these treated animals were isolated at 6 dpi, enriched by Percoll, and analyzed by flow cytometry. Cells were stained with Live/Dead aqua and with antibodies to CD3, CD4, CD11b, Ly6C, and Ly6G. (A) Representative scatter plots showing CD45 and CD4 expression, gated on live cells. Numbers in scatter plots indicate CD4⁺ population percentages of total live cells. Bar charts show average numbers of total leukocytes (left) and CD4⁺ T cell infiltrates (right). (B) Representative scatter plots showing CD11b and Ly6G expression gated on live CD45⁺ cells. Numbers in scatter plots indicate the percentages of cells in respective quadrants of total live CD45⁺ cells. Bar charts show average numbers of total myeloid cells (left) and neutrophil infiltrates (right). (C) Representative scatter plots showing CD11b and Ly6C expression gated on live CD45⁺ cells. Numbers in scatter plots indicate the percentages of cells in respective quadrants of total live CD45⁺ cells. Bar charts show average number of Ly6C⁻ macrophage (left) and Ly6C⁺ macrophage (right) infiltrates. All data are means and SD from 3 independent experiments. Statistical analysis was performed using one-way ANOVA across all CHIKV-infected groups, followed by Dunnett's posttest comparing to the PBS-CHIKV group. ***, $P < 0.0001$ (IL-2 Ab Cx CD4⁺ T cells).

Biosciences) and anti-CD25 (eBioscience). Intracellular staining of Foxp3 was done using a Foxp3 staining buffer set (eBioscience) and anti-Foxp3 following the manufacturer's instructions. Data were acquired using a BD LSRFortessa cell analyzer. Dead cells and duplets were excluded in all analyses using forward and side scatter gating. Results were analyzed with FlowJo version X software (Tree Star, Inc.).

Histology. Mice were anesthetized with ketamine (150 mg/kg)-xylazine (10 mg/kg) and perfused by intracardiac injection with PBS followed by 4% paraformaldehyde. Tissues were stored in 4% paraformaldehyde, decalcified, and embedded in paraffin wax before 5- μ m-thick sections were cut. Hematoxylin and eosin (H&E) staining was done using established protocols as previously described (16, 33). ImageJ software (National Institutes of Health) was used for binary image conversion of histological images and for particle analysis (average number of particles per 30,000 square pixels of area selected) to determine the number of cellular infiltrates (35).

Depletion of Tregs. Depletion of regulatory T cell (DEREG) (36) mice were treated with IL-2 Ab Cx for 3 days, following which 0.5 μ g of diphtheria toxin (DT) was administered daily to each mouse for 2 days. Treg depletion was checked by taking 10 μ l of blood from the tail vein, staining it with antibodies against CD4, CD25, and Foxp3, and analyzing the result with flow cytometry. Mice were then infected with CHIKV-SGP011 s.c., and depletion of Tregs was maintained by DT administration every other day.

Cell isolation from spleens, pLN, and joint footpads. Spleens, popliteal lymph nodes (pLN), and joint footpads of CHIKV-infected mice were harvested at 6 dpi. Isolation of splenocytes and joint footpad cells was

carried out as previously described (16). pLN cells were isolated by first incubating pLN in digestion medium containing 2 U/ml dispase (Invitrogen), 20 mg/ml collagenase IV (Sigma-Aldrich) and 50 mg/ml DNase I (Roche Applied Science) mix in complete RPMI for 30 min. Cells were then released from the digested pLN into the medium by gentle pipetting motions. Cell suspensions were then passed through a 70- μ m nylon cloth (Sefar), washed, and resuspended in complete RPMI. Cell count and viability were determined using trypan blue (Sigma).

Immunophenotyping of leukocytes by flow cytometry. Isolated cells from spleens, joint footpads, and pLN were first stained with a Live/Dead fixable aqua dead cell staining kit (1:400) (Life Technologies) for 20 min. Cells were then washed and resuspended in 50 μ l blocking buffer (1% rat and hamster serum in PBS). Staining was performed using anti-CD45 (BD Pharmingen), anti-CD4 (BD Pharmingen), anti-CD8 (eBioscience), anti-CD25 (eBioscience), anti-CD11b (eBioscience), anti-Ly6C (eBioscience), and anti-Ly6G (BioLegend) antibodies for 20 min. Stained cells were then washed with PBS and fixed using IC fixation buffer (eBioscience). Intracellular staining of anti-Foxp3 (eBioscience) was done according to the manufacturer's instructions. Data acquisition and analyses were done as described above.

IFN- γ ELISpot assay. Polyvinylidene difluoride (PVDF) membrane plates (Millipore) were humidified with 35% ethanol and washed with water. Wells were coated with anti-gamma interferon (IFN- γ) capture antibody (clone AN18; Mabtech) overnight at 4°C. Mice were sacrificed at 6 dpi, and joint footpad and pLN cells were isolated as described above. Splenocytes, joint footpad cells, and pLN cells were added at 2×10^5 , 2.5×10^4 , and 5×10^4 cells per well, respectively. *Ex vivo* CD4⁺ enrich-

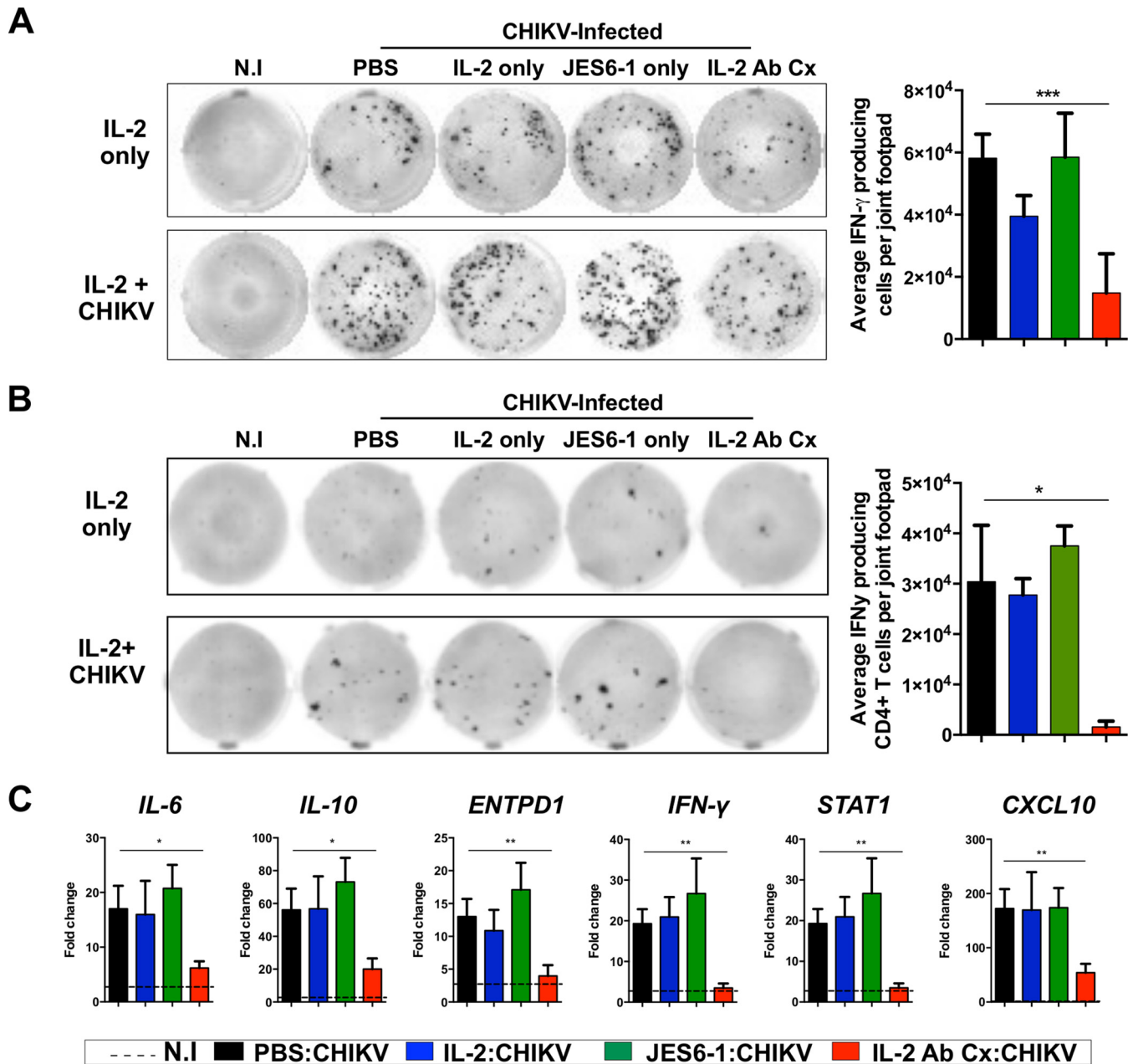


FIG 4 Pretreatment with IL-2 Ab Cx reduces production of proinflammatory cytokines in joint footpads of CHIKV-infected mice. WT mice ($n = 5$ per group) were infected s.c. with 10^6 PFU CHIKV-SGP011 after treatment with PBS, IL-2 only, JES6-1 only, or IL-2 Ab Cx. Cells were stimulated with either IL-2 only or IL-2 plus CHIKV. ELISpot was performed in quadruplicate to detect for CHIKV-specific IFN- γ -producing cells. (A and B) Representative images of ELISpot wells depicting the number of IFN- γ -producing cells in total cells (A) and enriched CD4⁺ T cells (B) from joint footpads. Bar charts show average numbers of IFN- γ -producing cells per infected joint footpad after subtraction of the background of the IL-2-only stimulation control. (C) mRNA was extracted from joint footpads, and qRT-PCR was performed to detect the expression of IL-6, IL-10, ENTPD1, IFN- γ , STAT1, and CXCL10. Statistical analysis was done using one-way ANOVA across all CHIKV-infected groups, followed by Dunnett's posttest comparing to the PBS-CHIKV group. Data are means and SD from three independent experiments. *, $P = 0.0127$ (IL-2 Ab Cx IL-6) or 0.0113 (IL-2 Ab Cx IL-10); **, $P = 0.0037$ (IL-2 Ab Cx ENTPD1), 0.0036 (IL-2 Ab Cx IFN- γ), 0.0032 (IL-2 Ab Cx STAT1), or 0.0067 (IL-2 Ab Cx CXCL10); ***, $P = 0.0008$ (IL-2 Ab Cx IFN- γ -producing cells per joint footpad) or 0.0126 (IL-2 Ab Cx IFN- γ -producing CD4⁺ T cells per joint footpad).

ment was performed using a mouse CD4⁺ T cell isolation kit II (Miltenyi Biotec) according to the manufacturer's instructions. Stimulation of CHIKV-specific T cells was done in complete RPMI containing 30 U/ml IL-2 and 1.5×10^6 VeroE6-derived SGP011 virions per well. Complete RPMI containing 30 U/ml IL-2 was included as a negative control. For all wells containing joint footpad cells, 1.5×10^5 splenocytes from NI mice

were added to serve as antigen-presenting cells (APCs). The plates were incubated at 37°C and 5% CO₂ for 18 h. After incubation, cells were removed and wells were washed six times using PBS. Spot detection was done using a mouse IFN- γ enzyme-linked immunospot (ELISpot) kit with alkaline phosphatase (ALP) (Mabtech) following the manufacturer's instructions.

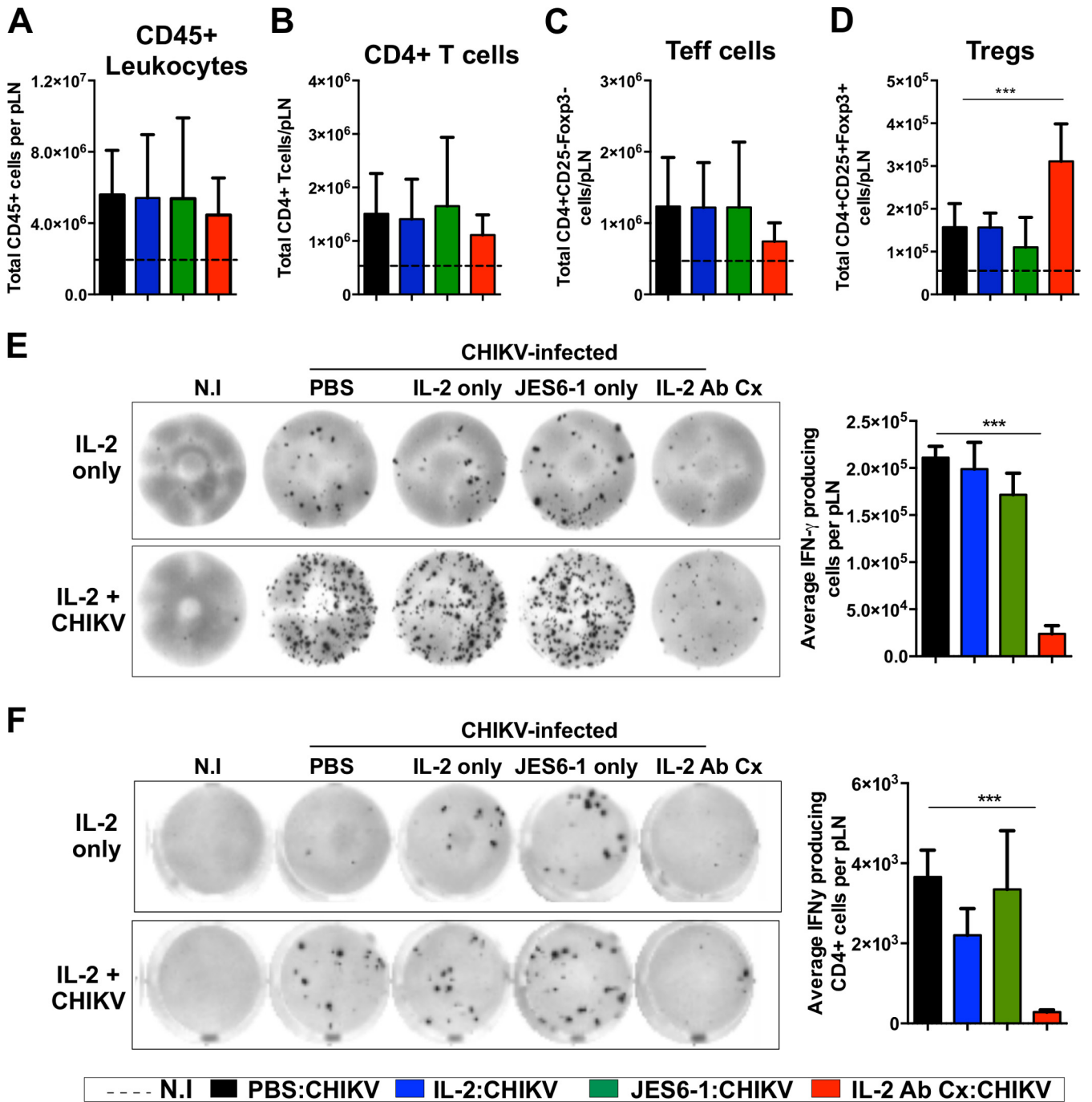


FIG 5 Pretreatment with IL-2 Ab Cx reduces the frequency of CHIKV-specific responses in pLN. WT mice ($n = 5$ per group) were infected s.c. with 10^6 PFU CHIKV-SGP011 after treatment with PBS, IL-2 only, JES6-1 only, or IL-2 Ab Cx. Cells from draining pLN were isolated at 6 dpi and analyzed using flow cytometry. (A through D) The bar charts show CD45⁺ T cells (A), CD4⁺ T cells (B), CD4⁺ Teff cells (C), and CD4⁺ Tregs (D) per pLN. Cells were stimulated with either IL-2 only or IL-2 plus CHIKV. ELISpot was performed in quadruplicate to detect for CHIKV-specific IFN- γ -producing cells. (E and F) Representative images of ELISpot wells depicting the number of IFN- γ -producing cells in total cells (E) and enriched CD4⁺ T cells (F) from pLN. The bar charts show the average numbers of IFN- γ -producing cells per pLN after subtraction of the background of the IL-2-only stimulation control. Statistical analysis was done using one-way ANOVA across all CHIKV-infected groups, followed by Dunnett's posttest comparing to the PBS-CHIKV group. Data are means and SD from three independent experiments. ***, $P < 0.0001$ (IL-2 Ab Cx Tregs per pLN), 0.0008 (IL-2 Ab Cx IFN- γ -producing cells per pLN), or 0.0007 (IL-2 Ab Cx IFN- γ -producing CD4⁺ T cells per pLN).

In vitro T cell proliferation. Cells were isolated from pLN as described above. *Ex vivo* CD4⁺ enrichment was performed using an EasySep mouse CD4⁺ cell enrichment kit (Stemcell) according to the manufacturer's instructions. Enriched CD4⁺ T cells were then labeled

with 2.5 μ M carboxyfluorescein succinimidyl ester (CFSE for 10 min at 37°C in the dark. Labeled cells were plated at 1×10^5 cells/well and stimulated with either anti-CD3/CD28 Dynabeads (Life Technologies) or CD4-depleted splenocytes from naive mice pulsed with 1.5×10^6

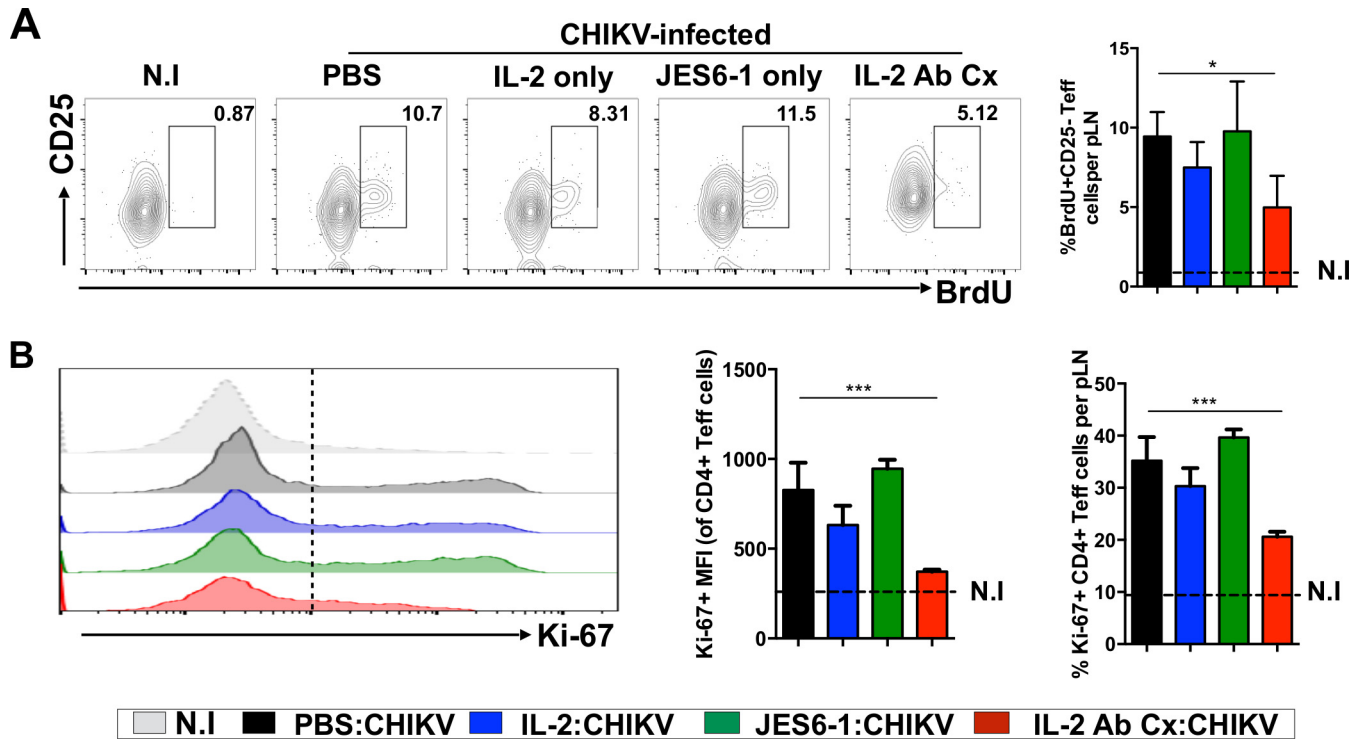


FIG 6 Pretreatment with IL-2 Ab Cx perturbs proliferation of activated CD4⁺ T eff cells. WT mice ($n = 5$ per group) were infected s.c. with 10^6 PFU CHIKV-SGP011 after treatment with PBS, IL-2 only, JES6-1 only, or IL-2 Ab Cx. (A) Representative scatterplot of CD25 expression and BrdU staining of T eff cells. BrdU was injected i.p. into mice daily for 2 days before euthanasia to detect proliferating cells. Cells isolated from draining pLN at 6 dpi were isolated for flow cytometry and gated on CD4⁺ T eff cells for analysis. The bar chart shows the average number of BrdU⁺ CD25⁺ T eff cells per pLN. (B) Histogram showing Ki-67 expression on CD4⁺ T eff cells (left) and bar charts showing mean fluorescence intensity (MFI) of Ki-67 on T eff cells (middle) and average percentage of Ki-67⁺ T eff cells (right). Statistical analysis was done using one-way ANOVA across all CHIKV-infected groups, followed by Dunnett's posttest comparing to the PBS-CHIKV group. Data are means and SD from three independent experiments. *, $P = 0.0324$ (IL-2 Ab Cx percentage BrdU⁺ T eff cells); ***, $P < 0.0001$ (IL-2 Ab Cx Ki-67 MFI and IL-2 Ab Cx percentage Ki-67⁺ T eff cells).

SGP011 virions per well. Cells were then incubated at 37°C for 4 days.

Statistical analyses. All statistical analyses were performed using GraphPad Prism 6. All analyses between the PBS-CHIKV, IL-2-CHIKV, JES6-1-CHIKV, and IL-2 Ab Cx-CHIKV groups were done using one-way analysis of variance (ANOVA) followed by Dunnett's multiple-comparison test comparing all other groups to the PBS-CHIKV group. Comparison between IL-2 Ab Cx with Treg depletion and IL-2 Ab Cx without depletion were done using an unpaired t test. Comparison between particle analysis of the PBS-CHIKV and IL-2 Ab Cx-CHIKV groups was done using a Mann-Whitney U test. A P value of less than 0.05 is considered statistically significant.

RESULTS

Tregs limit CHIKV-induced joint pathology. In order to assess if Tregs have a role in CHIKV-induced pathology, we made use of an *in vivo* method that allows the selective expansion of Tregs by administering IL-2 to form a complex with the anti-IL-2 antibody JES6-1, termed IL-2 Ab Cx (29). PBS, IL-2 only, or JES6-1 only was administered to mice prior to CHIKV infection as an experimental control (referred to as infected control groups). A significant increase in the proportion of circulating Tregs was observed only with IL-2 Ab Cx treatment (Fig. 1A) (29). This treatment was highly effective, as it increased the average frequency of Tregs in the blood from less than 10% to nearly 70% (Fig. 1A). Furthermore, the expanded Tregs were also activated, as indicated by high CD25 expression (Fig. 1A). The impact of Treg expansion on

CHIKV infection was next explored in mice pretreated with PBS (control), IL-2, JES6-1, or IL-2 Ab Cx for 3 days followed by virus inoculation into the footpad of the hind limb (27). Viremia and joint footpad swelling were monitored daily (Fig. 1B to E). Compared to noninfected (NI) mice, CHIKV infection resulted in substantial swelling of the joint that peaked at 6 days postinfection (dpi) (Fig. 1B and C). Differences were not observed within the control groups of CHIKV-infected mice (Fig. 1B and C). However, a marked reduction in swelling of the joint footpad was observed in mice pretreated with IL-2 Ab Cx, especially at 6 dpi (Fig. 1B and C). Notably, these mice also recovered faster, with undetectable levels of swelling by 8 dpi, than the other control groups, where swelling subsided only after 14 dpi (Fig. 1C).

The action of Tregs on reducing joint pathology did not have any effect on virus clearance, as differences in viral load were not observed between IL-2 Ab Cx-treated mice and CHIKV-infected control groups (Fig. 1D and E). Tissue sections of infected joint footpad were obtained for histological assessments, where PBS-treated CHIKV-infected mice exhibited typical necrotizing myositis with massive immune infiltrates as well as extensive edema (18, 37) in the loose connective tissue layer of the dermis layer (Fig. 1F). However, treatment with IL-2 Ab Cx markedly reduced edema within the dermis layer (Fig. 1F).

To ascertain that the reduced pathology observed in the IL-2 Ab Cx-treated mice was caused by the suppressive activity of Tregs

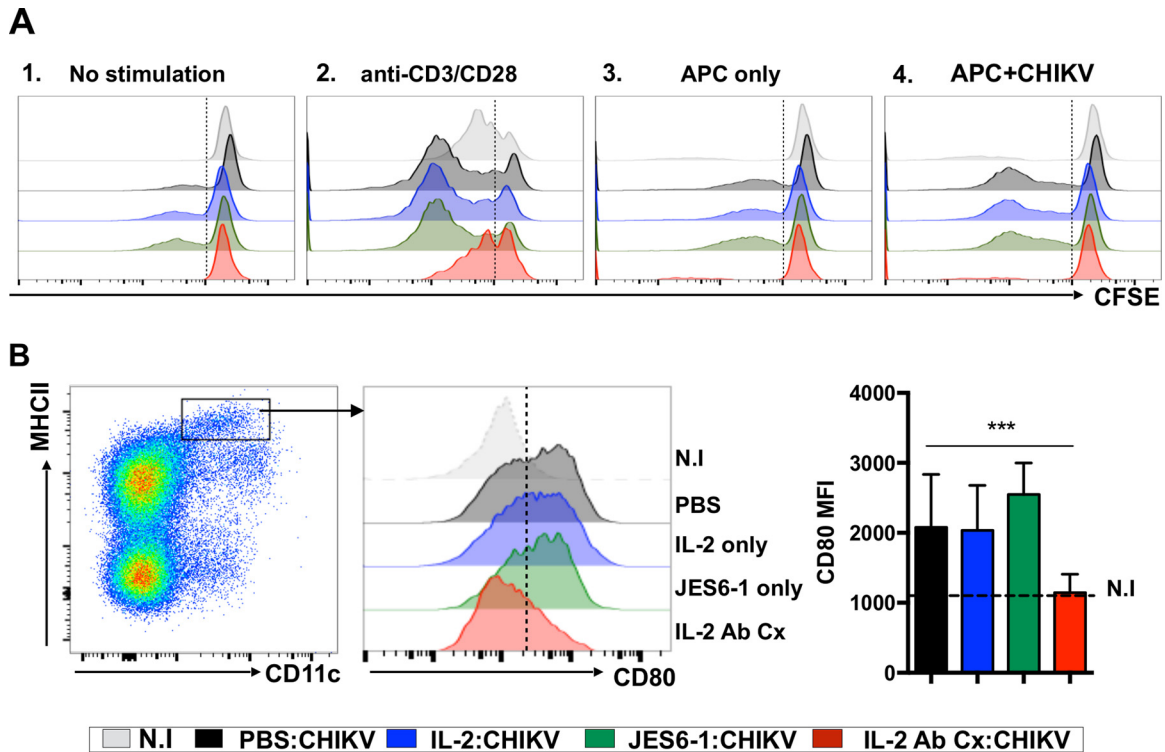


FIG 7 Pretreatment with IL-2 Ab Cx prevents proliferation of activated CHIKV-specific CD4⁺ T cells in draining lymph nodes. WT mice ($n = 5$ per group) were infected s.c. with 10^6 PFU CHIKV-SGP011 after treatment with PBS, IL-2 only, JES6-1 only, or IL-2 Ab Cx. Cells were isolated from draining pLN on 6 dpi. (A) Representative histogram illustrating CFSE dilution in stimulated T cells. Splenocytes from NI mice were depleted of CD4⁺ T cells and used as antigen-presenting cells (APCs). Enriched CD4⁺ T cells were depleted of Tregs, labeled with CFSE, and stimulated for 4 days with medium only, anti-CD3/CD28 Dynabeads, APCs only, or CHIKV-pulsed APCs. (B) Representative scatter plot (left) showing major histocompatibility complex class II (MHCII) and CD11c expression gated on total live CD45⁺ leukocytes from pLN. The boxed area corresponds to inflammatory DCs, which were further analyzed for CD80 expression, as shown in the histogram plot (middle). The bar chart (right) shows CD80 expression on inflammatory DCs. Statistical analysis was done using one-way ANOVA across all CHIKV-infected groups, followed by Dunnett's posttest comparing to the PBS-CHIKV group. Data are means and SD from two independent experiments. ***, $P = 0.0007$ (IL-2 Ab Cx CD80).

and not due to a direct impact of the IL-2 Ab Cx on the effector cells, DEREK mice were explored (36). These mice express diphtheria toxin receptor (DTR) under the control of Foxp3 promoter, which allows the specific ablation of Tregs with DT administration (Fig. 2A). In the absence of DT, treatment with IL-2 Ab Cx protected the CHIKV-infected DEREK mice from pronounced joint swelling (Fig. 2B). However, this protection was completely lost upon depletion of Tregs with DT (Fig. 2B). Joint swelling was comparable in DT-treated WT CHIKV-infected mice and in DT-treated DEREK mice with IL-2 Ab Cx treatment (Fig. 2B), verifying that the protection against CHIKV-induced swelling is mediated primarily by Tregs (Fig. 2).

Expansion of Tregs abrogates infiltration of Teff cells during CHIKV infection in pLN. In order to decipher how IL-2 Ab Cx ameliorates CHIKV-induced joint swelling, immune infiltrates at the site of infection were analyzed from harvested joint footpad samples isolated during the peak of inflammation at 6 dpi. A significant increase in the CD45⁺ leukocyte population was observed across all groups of CHIKV-infected mice (Fig. 3A). Flow cytometry analysis revealed that the infiltrates consisted mainly of CD11b⁺ myeloid cells that include macrophages and neutrophils (Fig. 3B). While CHIKV infection had no effect on the number of neutrophils (CD11b⁺ Ly6G⁺) (Fig. 3B), the number of infiltrating CD11b⁺ Ly6C⁺ inflammatory macrophages (Fig. 3C) in-

creased dramatically. While the expansion of Tregs did not impact the infiltration of macrophages induced by CHIKV infection, a striking selective effect was observed for CD4⁺ T cells infiltration on 6 dpi. While IL-2 and JES6-1 did not affect the influx of CD4⁺ T cells into the infected footpad, their infiltration was significantly reduced with IL-2 Ab Cx treatment (Fig. 3A).

IFN- γ ELISpot analysis on cells isolated from CHIKV-infected joint footpad samples further revealed that the reduced infiltrating CD4⁺ T cells correlated with a reduction of the antigen-specific CD4⁺ T cell response (Fig. 4A and B). Transcript analysis performed on total mRNA isolated from joint footpad cells indicated that although CHIKV infection induced high expression of proinflammatory genes, such as those encoding IL-6, IL-10, ENTPD1, IFN- γ , STAT1, and CXCL10, addition of IL-2 Ab Cx reversed this effect (Fig. 4C). A plausible explanation for this protective effect could be the interference by expanded Tregs on the priming of CHIKV-specific CD4⁺ Teff cells. To verify this, IFN- γ ELISpot and flow cytometry analyses were carried out on cells isolated from the draining pLN. Flow cytometry detected only minor differences in the absolute number of pLN cells (Fig. 5A to D). In contrast, IFN- γ ELISpot showed that CHIKV-specific stimulation yielded a high frequency of antigen-specific responses from total pLN and isolated CD4⁺ T cells in all CHIKV-infected groups except for the

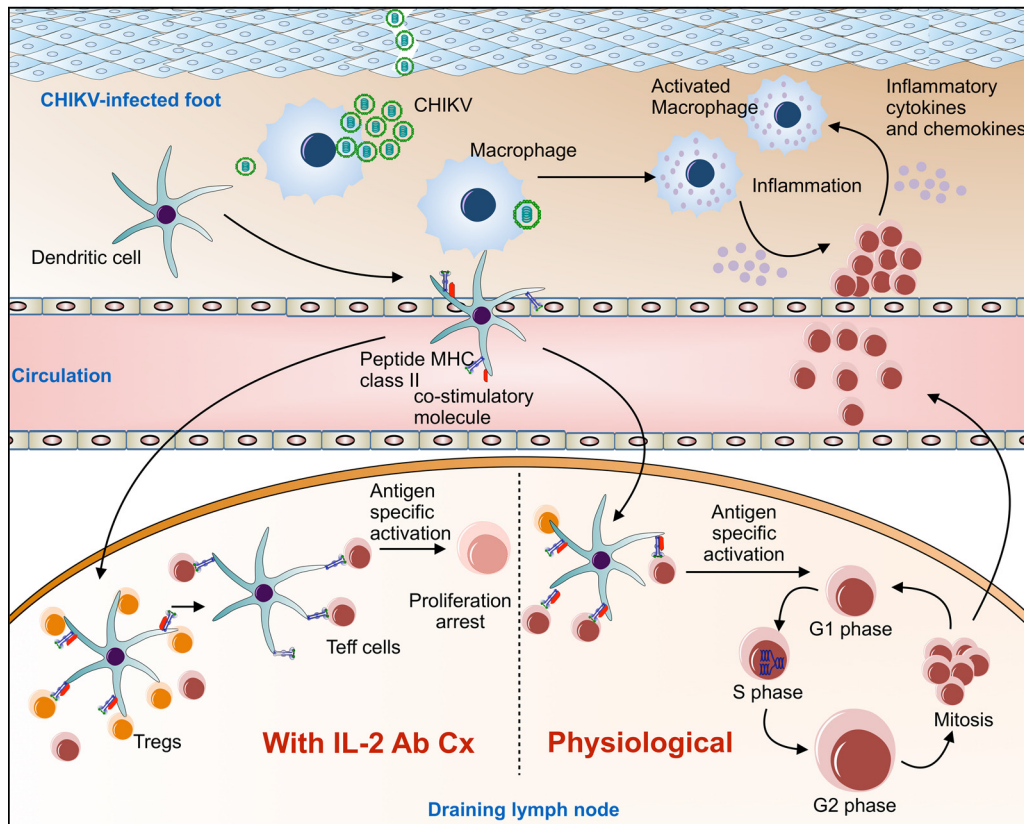


FIG 8 Proposed mechanism for reduction of CHIKV-induced pathology by IL-2 Ab Cx. Upon CHIKV infection in the joint footpad, resident sentinels such as macrophages and DCs sense the virus. Virus stimulation induces activation of macrophages, which secrete proinflammatory cytokines and chemokines to attract other immune cell populations. Meanwhile, DCs phagocytose viral particles and differentiate into mature migratory DCs to upregulate MHCII and costimulatory molecules. The matured DCs migrate to the draining pLN and present viral antigen to naive T cells. Upon interaction with their cognate antigen, naive T cells are activated into Teff cells and enter the cell cycle to expand clonally. These expanded CHIKV-specific Teff cells migrate toward the site of infection in response to secreted T cell chemokines. The presence of CHIKV-specific Teff cells exacerbates the proinflammatory milieu and gives rise to the inflamed joint pathology observed. In the event of IL-2 Ab Cx pretreatment, expanded Tregs will be present in large number in all the secondary lymphoid organs. As the mature DCs carrying CHIKV antigen arrive at the draining LN, Tregs compete with naive T cells to interact with these DCs. Treg-DC interaction then causes mature DCs to downregulate their costimulatory molecules and results in the DCs presenting CHIKV antigens to naive T cells in the absence of costimulatory signals. Activation of T cells without costimulation is likely to drive the T cells into G₁ arrest, resulting in anergy. Anergic T cells are not able to migrate to the site of infection in response to chemoattractants. Abrogation of CHIKV-specific Teff cells infiltration in the site of infection prevents exacerbation of proinflammatory environment, thus preventing the inflamed-joint pathology.

IL-2 Ab Cx-treated group (Fig. 5E and F). This suggests that generation of CHIKV-specific CD4⁺ Teff cells is likely to be perturbed in the presence of expanded Tregs.

Tregs block proliferation and differentiation of CHIKV-specific Teff cells. To further address how Tregs suppress the initial priming of CD4⁺ Teff cells in the pLN, bromodeoxyuridine (BrdU) was administered before the peak of joint swelling at 4 dpi and 5 dpi to detect *in vivo* proliferation of CD4⁺ Teff cells. About 10% of CD4⁺ Teff cells from CHIKV-infected PBS-treated control mice were BrdU⁺ (Fig. 6A), suggesting that these cells were actively proliferating in response to virus infection. On the other hand, Teff cells from IL-2 Ab Cx-treated mice had significantly lower detectable levels of BrdU⁺ cells (Fig. 6A). In order to confirm if the lack of BrdU uptake was due to a disruption in the proliferation of CD4⁺ Teff cells, Ki-67 staining was performed to assess cell cycle advancement (38). Draining pLN from CHIKV-infected control mice revealed that approximately 30% of CD4⁺ Teff cells expressed Ki-67, indicating active proliferation of these lymphocytes (Fig. 6B). However, only 20% of CD4⁺ Teff cells

from IL-2 Ab Cx-treated mice expressed Ki-67 (Fig. 6B). More importantly, Teff cells from the IL-2 Ab Cx-treated group showed significantly reduced Ki-67 detection compared to the CHIKV-infected control groups (Fig. 6B). Taken together, these findings suggest that CD4⁺ Teff cells with IL-2 Ab Cx treatment did proliferate but did not enter S phase (Fig. 6).

Tregs inhibit priming of CHIKV-specific Teff cells due to the induction of anergy. Finally, to address proliferation arrest (39–41), CD4⁺ Teff cells were isolated from pLN of CHIKV-infected mice on 6 dpi and challenged with either CHIKV-pulsed APCs or anti-CD3/CD28 Dynabeads. Tregs were depleted using anti-CD25 positive selection, as they are known to exhibit suppressive effects during mixed lymphocyte reactions (42). To monitor proliferation, isolated CD4⁺ Teff cells were labeled with carboxyfluorescein succinimidyl ester (CFSE), a tracking dye for proliferation (43). CD4⁺ Teff cells from all groups responded to nonspecific anti-CD3/CD28 stimulation (Fig. 7). While CD4⁺ Teff cells from IL-2 Ab Cx showed a weaker proliferation that was comparable to that in the NI group (Fig. 7A, panel 2), CHIKV-specific stimula-

tion did not (Fig. 7A, panel 4). Proliferation was observed only in the CHIKV-infected control groups, not in the IL-2 Ab Cx-treated mice (Fig. 7A, panel 4). This demonstrates that anergy induction is specific to CHIKV-specific CD4⁺ T cells and not due to a global shutdown of T cell responses.

Flow cytometry was further performed to assess if the induction of anergy was due to a lack of costimulation on the APCs during T cell activation (39–41, 44–47). Although migratory dendritic cells (DCs) (CD11b⁺ CD11c⁺ MHCII^{hi}) (48) isolated from the draining pLN of CHIKV-infected control groups revealed a typical increase in CD80 (Fig. 7B), treatment with IL-2 Ab Cx resulted in a significant reduction of CD80 (Fig. 7B). These observations further substantiate the idea that Tregs disrupted the response of CHIKV-specific CD4⁺ T cells by altering the priming capacity of APCs (49–52).

DISCUSSION

Arboviral infections have illustrated the importance of T cells in regulating disease pathology (53–55). CD8⁺ T cells were demonstrated to mediate encephalitis during Murray Valley encephalitis virus (MVE) infection (54). Cross-reactive CD4⁺ T cells were found to exacerbate dengue hemorrhagic fever (DHF) during secondary infections (55), while CD8⁺ T cells have an ambivalent role, as they exhibit both protective and pathogenic effects in WNV-infected mice (56). More recently, CD4⁺ T cells were shown to be responsible in mediating CHIKV-induced pathology (16). While T cell-mediated immunopathology in arbovirus infections has been extensively reported (54, 55, 57, 58), information on the role of Tregs remains limited. Here, aberrant immune responses responsible for the development of CHIKV-induced immunopathology were controlled by selectively expanding Tregs *in vivo* through administering IL-2 Ab Cx prior to virus infection (29). The expansion and activation of Tregs led to the effective amelioration of the characteristic CHIKV-induced joint swelling. The reduced inflamed joint pathology was similar to that observed in CHIKV-infected CD4^{-/-} mice, where a decline in viremia was not affected by the absence of CD4⁺ T cells (16).

Further characterization of the action of these expanded Tregs during CHIKV infection established that Tregs selectively inhibit CD4⁺ T cells. IFN- γ ELISpot performed on splenocytes and cells from draining pLN isolated from IL-2 Ab Cx-treated CHIKV-infected mice resulted in a sharp reduction in the frequency of CHIKV-specific CD4⁺ T cells. Consequently, only a low number of CHIKV-specific CD4⁺ T cells could migrate into infected tissues to maintain inflammation and inflict further damage. Notably, the influx of other immune subsets, such as macrophages and CD8⁺ T cells, was not affected, indicating no impairment in the overall immune response. BrdU and Ki-67 analysis suggested cell cycle arrest in CD4⁺ T cells, a hallmark feature of anergic T cells (59–61). In line with this, a reduction in the level of CD80 in migratory DCs further suggested the indirect immunosuppressive effect of Tregs on T cells via the effect of Tregs on APCs (49–52). During virus infection, viral antigens are picked up by tissue-resident DCs that mature into migratory DCs and are transported to the draining LN to prime virus-specific T cells (62). These activated T cells then migrate back to the site of infection and exacerbate the proinflammatory microenvironment. Findings in this study suggest that Treg expansion perturbs this inflammatory cycle by interacting with the APCs to inhibit the upregulation of costimulatory mole-

cules that cause induction of anergy due to incomplete T cell activation in the primed cells (Fig. 8).

The protective role of Tregs in reducing immunopathology seen in this study could be further extended to other clinically important arboviruses such as O'nyong-nyong virus (ONNV), Ross river virus (RRV), and Dengue virus (DENV) (63–65) as a means to prevent or reduce pathology (53, 66). Nonetheless, observations in this study imply that pharmaceutical immunosuppressants blocking T cell activation and/or proliferation have a wealth of therapeutic potential (67) and could represent an alternative way to control virus-induced pathology during the acute phase of infection.

ACKNOWLEDGMENTS

We thank Anis Larbi and the S μ gN Flow Cytometry core facility for assistance with cytometry analysis. We are also grateful to the Mutant Mouse Collection (S μ gN, A*STAR) and A*STAR Biological Resource Centre (BRC) for their assistance with breeding and supply of mice used in this study. We also thank the Advanced Molecular Pathology Laboratory (IMCB, A*STAR) for performing the histology work. We acknowledge Kai-Er Eng from S μ gN for assistance with manuscript editing.

The study was supported by the Biomedical Research Council, A*STAR. Wendy W. L. Lee was supported by a postgraduate scholarship from the NUS Graduate School for Integrative Science and Engineering (NGS). Teck-Hui Teo was supported by an A*STAR postgraduate scholarship. Fok-Moon Lum was supported by the President's Graduate Fellowship from the Yong Loo Lin School of Medicine, National University of Singapore (Singapore).

The funders had no role in study design, data collection and analysis, decision to publish, or preparation of the manuscript. We declare that no conflict of interest exists.

REFERENCES

- Kennedy A, Fleming J, Solomon L. 1979. Chikungunya viral arthropathy: a clinical description. *J Rheumatol* 7:231–236.
- Pfefferkorn ER, Shapiro D. 1974. Reproduction of togaviruses, p 171–230. *In* Fraenkel-Conrat H, Wagner RR (ed), *Reproduction: small and intermediate RNA viruses*. Springer, New York, NY.
- Renault P, Solet J-L, Sissoko D, Balleydier E, Larrieu S, Filleul L, Lassalle C, Thiria J, Rachou E, de Valk H, Ilef D, Ledrans M, Quatre-sous I, Quenel P, Pierre V. 2007. A major epidemic of chikungunya virus infection on Réunion Island, France, 2005–2006. *Am J Trop Med Hyg* 77:727–731.
- Pialoux G, Gaüzère B-A, Jauréguiberry S, Strobel M. 2007. Chikungunya, an epidemic arbovirolosis. *Lancet Infect Dis* 7:319–327. [http://dx.doi.org/10.1016/S1473-3099\(07\)70107-X](http://dx.doi.org/10.1016/S1473-3099(07)70107-X).
- Powers AM, Logue CH. 2007. Changing patterns of chikungunya virus: re-emergence of a zoonotic arbovirus. *J Gen Virol* 88:2363–2377. <http://dx.doi.org/10.1099/vir.0.82858-0>.
- Rezza G, Nicoletti L, Angelini R, Romi R, Finarelli AC, Panning M, Cordioli P, Fortuna C, Boros S, Magurano F, Silvi G, Angelini P, Dottori M, Ciufolini MG, Majori GC, Cassone A. 2007. Infection with chikungunya virus in Italy: an outbreak in a temperate region. *Lancet* 370:1840–1846. [http://dx.doi.org/10.1016/S0140-6736\(07\)61779-6](http://dx.doi.org/10.1016/S0140-6736(07)61779-6).
- Grandadam M, Caro V, Plumet S, Thiberge JM, Souarès Y, Failloux AB, Tolou HJ, Budelot M, Cosserat D, Leparç-Goffart I, Desprès P. 2011. Chikungunya virus, southeastern France. *Emerg Infect Dis* 17:910. <http://dx.doi.org/10.3201/eid1705.101873>.
- Cagney H. 2014. Infectious disease surveillance update. *Lancet Infect Dis* 14:377. [http://dx.doi.org/10.1016/S1473-3099\(14\)70762-5](http://dx.doi.org/10.1016/S1473-3099(14)70762-5).
- Leparç-Goffart I, Nougairède A, Cassadou S, Prat C, de Lamballerie X. 2014. Chikungunya in the Americas. *Lancet* 383:514. [http://dx.doi.org/10.1016/S0140-6736\(14\)60185-9](http://dx.doi.org/10.1016/S0140-6736(14)60185-9).
- Pan American Health Organization. 31 Oct 2014. Number of reported cases of chikungunya fever in the Americas, by country or territory. http://www.paho.org/hq/index.php?option=com_docman&task=doc_download&Itemid=&gid=27998&lang=en. Accessed 6 November 2014.

11. Roth A, Hoy D, Horwood PF, Ropa B, Hancock T, Guillaumot L, Rickart K, Frison P, Pavlin B, Souares Y. 2014. Preparedness for threat of chikungunya in the Pacific. *Emerg Infect Dis*, vol 20. <http://dx.doi.org/10.3201/eid2008.130696>.
12. Simon F, Parola P, Grandadam M, Fourcade S, Oliver M, Brouqui P, Hance P, Kraemer P, Mohamed AA, de Lamballerie X, Charrel R, Tolou H. 2007. Chikungunya infection: an emerging rheumatism among travelers returned from Indian Ocean islands. Report of 47 cases. *Medicine* 86:123–137. <http://dx.doi.org/10.1097/MD.0b013e31806010a5>.
13. Chow A, Her Z, Ong EKS, Chen J-M, Dimatatac F, Kwek DJC, Barkham T, Yang H, Rénia L, Leo Y-S, Ng LFP. 2011. Persistent arthralgia induced by chikungunya virus infection is associated with interleukin-6 and granulocyte macrophage colony-stimulating factor. *J Infect Dis* 203:149–157. <http://dx.doi.org/10.1093/infdis/jiq042>.
14. Borgherini G, Poubeau P, Jossaume A, Goux A, Cotte L, Michault A, Arvin-Berod C, Paganin F. 2008. Persistent arthralgia associated with chikungunya virus: a study of 88 adult patients on Reunion Island. *Clin Infect Dis* 47:469–475. <http://dx.doi.org/10.1086/590003>.
15. Ng LFP, Chow A, Sun Y-J, Kwek DJC, Lim P-L, Dimatatac F, Ng L-C, Ooi E-E, Choo K-H, Her Z, Kourilsky P, Leo Y-S. 2009. IL-1 β , IL-6, and RANTES as biomarkers of chikungunya severity. *PLoS One* 4:e4261. <http://dx.doi.org/10.1371/journal.pone.0004261>.
16. Teo TH, Lum FM, Claser C, Lulla V, Lulla A, Merits A, Rénia L, Ng LFP. 2013. A pathogenic role for CD4+ T cells during chikungunya virus infection in mice. *J Immunol* 190:259–269. <http://dx.doi.org/10.4049/jimmunol.1202177>.
17. Hoarau J-J, Jaffar Bandjee M-C, Krejbich Trotot P, Das T, Li-Pat-Yuen G, Dassa B, Denizot M, Guichard E, Ribera A, Henni T, Tallet F, Moiton MP, Gauzère BA, Bruniquet S, Jaffar Bandjee Z, Morbidelli P, Martigny G, Jolivet M, Gay F, Grandadam M, Tolou H, Vieillard V, Debré P, Autran B, Gasque P. 2010. Persistent chronic inflammation and infection by chikungunya arthritogenic alphavirus in spite of a robust host immune response. *J Immunol* 184:5914–5927. <http://dx.doi.org/10.4049/jimmunol.0900255>.
18. Morrison TE, Oko L, Montgomery SA, Whitmore AC, Lotstein AR, Gunn BM, Elmore SA, Heise MT. 2011. A mouse model of chikungunya virus-induced musculoskeletal inflammatory disease: evidence of arthritis, tenosynovitis, myositis, and persistence. *Am J Pathol* 178:32–40. <http://dx.doi.org/10.1016/j.ajpath.2010.11.018>.
19. Nakaya HI, Gardner J, Poo Y-S, Major L, Pulendran B, Suhrbier A. 2012. Gene profiling of Chikungunya virus arthritis in a mouse model reveals significant overlap with rheumatoid arthritis. *Arthritis Rheum* 64:3553–3563. <http://dx.doi.org/10.1002/art.34631>.
20. Poo YS, Rudd PA, Gardner J, Wilson JAC, Larcher T, Colle M-A, Le TT, Nakaya HI, Warrilow D, Allcock R, Bielefeldt-Ohmann H, Schroder WA, Khromykh AA, Lopez JA, Suhrbier A. 2014. Multiple immune factors are involved in controlling acute and chronic chikungunya virus infection. *PLoS Negl Trop Dis* 8:e3354. <http://dx.doi.org/10.1371/journal.pntd.0003354>.
21. Lundgren A, Suri-Payer E, Enarsson K, Svennerholm A-M, Lundin BS. 2003. Helicobacter pylori-specific CD4+ CD25high regulatory T cells suppress memory T-cell responses to H. pylori in infected individuals. *Infect Immun* 71:1755–1762. <http://dx.doi.org/10.1128/IAI.71.4.1755-1762.2003>.
22. Suvas S, Azkur AK, Kim BS, Kumaraguru U, Rouse BT. 2004. CD4+CD25+ regulatory T cells control the severity of viral immunoinflammatory lesions. *J Immunol* 172:4123–4132. <http://dx.doi.org/10.4049/jimmunol.172.7.4123>.
23. Sakaguchi S, Sakaguchi N, Asano M, Itoh M, Toda M. 1995. Immunologic self-tolerance maintained by activated T cells expressing IL-2 receptor alpha-chains (CD25). Breakdown of a single mechanism of self-tolerance causes various autoimmune diseases. *J Immunol* 155:1151–1164.
24. McKinley L, Logar AJ, McAllister F, Zheng M, Steele C, Kolls JK. 2006. Regulatory T cells dampen pulmonary inflammation and lung injury in an animal model of Pneumocystis pneumonia. *J Immunol* 177:6215–6226. <http://dx.doi.org/10.4049/jimmunol.177.9.6215>.
25. Centers for Disease Control and Prevention. 3 Oct 2014. West Nile virus disease cases and presumptive viremic blood donors by state—United States. <http://www.cdc.gov/westnile/statsMaps/preliminaryMapsData/histatedate.html>. Accessed 7 Oct 2014.
26. Lanteri MC, Brien KM, Purtha WE, Cameron MJ, Lund JM, Owen RE, Heitman JW, Custer B, Hirschhorn DF, Tobler LH, Kiely N, Prince HE, Ndhlovu LC, Nixon DF, Kamel HT, Kelvin DJ, Busch MP, Rudensky AY, Diamond MS, Norris PJ. 2009. Tregs control the development of symptomatic West Nile virus infection in humans and mice. *J Clin Invest* 119:3266–3277. <http://dx.doi.org/10.1172/JCI39387>.
27. Gardner J, Anraku I, Le TT, Larcher T, Major L, Roques P, Schroder WA, Higgs S, Suhrbier A. 2010. Chikungunya virus arthritis in adult wild-type mice. *J Virol* 84:8021–8032. <http://dx.doi.org/10.1128/JVI.02603-09>.
28. Sakaguchi S, Yamaguchi T, Nomura T, Ono M. 2008. Regulatory T cells and immune tolerance. *Cell* 133:775–787. <http://dx.doi.org/10.1016/j.cell.2008.05.009>.
29. Boyman O, Kovar M, Rubinstein MP, Surh CD, Sprent J. 2006. Selective stimulation of T cell subsets with antibody-cytokine immune complexes. *Science* 311:1924–1927. <http://dx.doi.org/10.1126/science.1122927>.
30. Her Z, Malleret B, Chan M, Ong EKS, Wong S-C, Kwek DJC, Tolou H, Lin RTP, Tambyah PA, Rénia L, Ng LFP. 2010. Active infection of human blood monocytes by chikungunya virus triggers an innate immune response. *J Immunol* 184:5903–5913. <http://dx.doi.org/10.4049/jimmunol.0904181>.
31. Kam YW, Lum FM, Teo TH, Lee WWL, Simarmata D, Harjanto S, Chua CL, Chan YF, Wee JK, Chow A, Lin RTP, Leo YS, Le Grand R, Sam IC, Tong JC, Roques P, Wiesmüller KH, Rénia L, Röttschke O, Ng LFP. 2012. Early neutralizing IgG response to chikungunya virus in infected patients targets a dominant linear epitope on the E2 glycoprotein. *EMBO Mol Med* 4:330–343. <http://dx.doi.org/10.1002/emmm.201200213>.
32. Lum FM, Teo TH, Lee WWL, Kam Y-W, Rénia L, Ng LFP. 2013. An essential role of antibodies in the control of chikungunya virus infection. *J Immunol* 190:6295–6302. <http://dx.doi.org/10.4049/jimmunol.1300304>.
33. Teng T-S, Foo S-S, Simamarta D, Lum F-M, Teo T-H, Lulla A, Yeo NKW, Koh EGL, Chow A, Leo Y-S, Merits A, Chin K-C, Ng LFP. 2012. Viperin restricts chikungunya virus replication and pathology. *J Clin Invest* 122:4447–4460. <http://dx.doi.org/10.1172/JCI63120>.
34. Plaskon NE, Adelman ZN, Myles KM. 2009. Accurate strand-specific quantification of viral RNA. *PLoS One* 4:e7468. <http://dx.doi.org/10.1371/journal.pone.0007468>.
35. Schneider CA, Rasband WS, Eliceiri KW. 2012. NIH Image to ImageJ: 25 years of image analysis. *Nat Methods* 9:671–675. <http://dx.doi.org/10.1038/nmeth.2089>.
36. Lahl K, Sparwasser T. 2011. In vivo depletion of FoxP3+ Tregs using the DEREK mouse model, p 157–172. In Kassiotis G, Liston A (ed), *Regulatory T cells*, vol 707. Humana Press, Totowa, NJ.
37. Rulli NE, Rolph MS, Srikiatkachorn A, Anantapreecha S, Guglielmotti A, Mahalingam S. 2011. Protection from arthritis and myositis in a mouse model of acute chikungunya virus disease by bindarit, an inhibitor of monocyte chemotactic protein-1 synthesis. *J Infect Dis* 204:1026–1030. <http://dx.doi.org/10.1093/infdis/jir470>.
38. Endl E, Steinbach P, Knüchel R, Hofstädter F. 1997. Analysis of cell cycle-related Ki-67 and p120 expression by flow cytometric BrdU-Hoechst/7AAD and immunolabeling technique. *Cytometry* 29:233–241. [http://dx.doi.org/10.1002/\(SICI\)1097-0320\(19971101\)29:3<233::AID-CYTO6>3.0.CO;2-C](http://dx.doi.org/10.1002/(SICI)1097-0320(19971101)29:3<233::AID-CYTO6>3.0.CO;2-C).
39. Schwartz R. 1990. A cell culture model for T lymphocyte clonal anergy. *Science* 248:1349–1356. <http://dx.doi.org/10.1126/science.2113314>.
40. Schwartz RH. 1996. Models of T cell anergy: is there a common molecular mechanism? *J Exp Med* 184:1–8. <http://dx.doi.org/10.1084/jem.184.1.1>.
41. Fathman CG, Lineberry NB. 2007. Molecular mechanisms of CD4+ T-cell anergy. *Nat Rev Immunol* 7:599–609. <http://dx.doi.org/10.1038/nri2131>.
42. Venken K, Thewissen M, Hellings N, Somers V, Hensen K, Rummens J-L, Stinissen P. 2007. A CFSE based assay for measuring CD4+CD25+ regulatory T cell mediated suppression of auto-antigen specific and polyclonal T cell responses. *J Immunol Methods* 322:1–11. <http://dx.doi.org/10.1016/j.jim.2007.01.025>.
43. Lyons AB, Parish CR. 1994. Determination of lymphocyte division by flow cytometry. *J Immunol Methods* 171:131–137. [http://dx.doi.org/10.1016/0022-1759\(94\)90236-4](http://dx.doi.org/10.1016/0022-1759(94)90236-4).
44. Mahnke K, Ring S, Johnson TS, Schallenberg S, Schönfeld K, Storn V, Bedke T, Enk AH. 2007. Induction of immunosuppressive functions of dendritic cells in vivo by CD4+CD25+ regulatory T cells: role of B7-H3 expression and antigen presentation. *Eur J Immunol* 37:2117–2126. <http://dx.doi.org/10.1002/eji.200636841>.
45. Kuklina EM. 2013. Molecular mechanisms of T-cell anergy. *Biochemistry (Moscow)* 78:144–156. <http://dx.doi.org/10.1134/S000629791302003X>.
46. Boussiotis VA, Freeman GJ, Taylor PA, Berzovskaya A, Grass I, Blazar

- BR, Nadler LM. 2000. p27kip1 functions as an anergy factor inhibiting interleukin 2 transcription and clonal expansion of alloreactive human and mouse helper T lymphocytes. *Nat Med* 6:290–297. <http://dx.doi.org/10.1038/73144>.
47. Kang SM, Beverly B, Tran AC, Brorson K, Schwartz RH, Lenardo MJ. 1992. Transactivation by AP-1 is a molecular target of T cell clonal anergy. *Science* 257:1134–1138. <http://dx.doi.org/10.1126/science.257.5073.1134>.
 48. Vermaelen KY, Carro-Muino I, Lambrecht BN, Pauwels RA. 2001. Specific migratory dendritic cells rapidly transport antigen from the airways to the thoracic lymph nodes. *J Exp Med* 193:51–60.
 49. Hänig J, Lutz MB. 2008. Suppression of mature dendritic cell function by regulatory T cells in vivo is abrogated by CD40 licensing. *J Immunol* 180:1405–1413. <http://dx.doi.org/10.4049/jimmunol.180.3.1405>.
 50. Onishi Y, Fehervari Z, Yamaguchi T, Sakaguchi S. 2008. Foxp3+ natural regulatory T cells preferentially form aggregates on dendritic cells in vitro and actively inhibit their maturation. *Proc Natl Acad Sci U S A* 105:10113–10118. <http://dx.doi.org/10.1073/pnas.0711106105>.
 51. Misra N, Bayry J, Lacroix-Desmazes S, Kazatchkine MD, Kaveri SV. 2004. Cutting edge: human CD4+CD25+ T cells restrain the maturation and antigen-presenting function of dendritic cells. *J Immunol* 172:4676–4680. <http://dx.doi.org/10.4049/jimmunol.172.8.4676>.
 52. Cederbom L, Hall H, Ivars F. 2000. CD4+CD25+ regulatory T cells down-regulate co-stimulatory molecules on antigen-presenting cells. *Eur J Immunol* 30:1538–1543. [http://dx.doi.org/10.1002/1521-4141\(200006\)30:6<1538::AID-IMMU1538>3.0.CO;2-X](http://dx.doi.org/10.1002/1521-4141(200006)30:6<1538::AID-IMMU1538>3.0.CO;2-X).
 53. Suhrbier A, La Linn M. 2004. Clinical and pathologic aspects of arthritis due to Ross River virus and other alphaviruses. *Curr Opin Rheumatol* 16:374–379. <http://dx.doi.org/10.1097/01.bor.0000130537.76808.26>.
 54. Licon Luna RM, Lee E, Müllbacher A, Blanden RV, Langman R, Lobigs M. 2002. Lack of both Fas ligand and perforin protects from flavivirus-mediated encephalitis in mice. *J Virol* 76:3202–3211. <http://dx.doi.org/10.1128/JVI.76.7.3202-3211.2002>.
 55. Gagnon SJ, Ennis FA, Rothman AL. 1999. Bystander target cell lysis and cytokine production by dengue virus-specific human CD4+ cytotoxic T-lymphocyte clones. *J Virol* 73:3623–3629.
 56. Wang Y, Lobigs M, Lee E, Müllbacher A. 2003. CD8+ T cells mediate recovery and immunopathology in West Nile virus encephalitis. *J Virol* 77:13323–13334. <http://dx.doi.org/10.1128/JVI.77.24.13323-13334.2003>.
 57. King NJC, Getts DR, Getts MT, Rana S, Shrestha B, Kesson AM. 2007. Immunopathology of flavivirus infections. *Immunol Cell Biol* 85:33–42. <http://dx.doi.org/10.1038/sj.icb.7100012>.
 58. Kurane I, Ennis FE. 1992. Immunity and immunopathology in dengue virus infections. *Semin Immunol* 4:121–127.
 59. Powell JD, Lerner CG, Schwartz RH. 1999. Inhibition of cell cycle progression by rapamycin induces T cell clonal anergy even in the presence of costimulation. *J Immunol* 162:2775–2784.
 60. Rudd CE. 2006. Cell cycle ‘check points’ T cell anergy. *Nat Immunol* 7:1130–1132. <http://dx.doi.org/10.1038/ni1106-1130>.
 61. Jenkins MK. 1992. The role of cell division in the induction of clonal anergy. *Immunol Today* 13:69–73. [http://dx.doi.org/10.1016/0167-5699\(92\)90137-V](http://dx.doi.org/10.1016/0167-5699(92)90137-V).
 62. Lombardi G, Rizzo-Vasquez Y. 2008. Dendritic cells. Springer, New York, NY.
 63. Powers AM. 2013. Infection patterns and emergence of O’nyong’nyong virus, p 433–444. *In* Singh SK (ed), *Viral infections and global change*. John Wiley & Sons, Inc., New York, NY.
 64. Yu W, Mengersen K, Dale P, Mackenzie JS, Toloo G, Wang X, Tong S. 2014. Epidemiologic patterns of Ross River virus disease in Queensland, Australia, 2001–2011. *Am J Trop Med Hyg* 91:109–118. <http://dx.doi.org/10.4269/ajtmh.13-0455>.
 65. San Martín JL, Brathwaite O, Zambrano B, Solórzano JO, Bouckenooghe A, Dayan GH, Guzmán MG. 2010. The epidemiology of dengue in the Americas over the last three decades: a worrisome reality. *Am J Trop Med Hyg* 82:128–135. <http://dx.doi.org/10.4269/ajtmh.2010.09-0346>.
 66. Suhrbier A, Jaffar-Bandjee M-C, Gasque P. 2012. Arthritogenic alphaviruses—an overview. *Nat Rev Rheumatol* 8:420–429. <http://dx.doi.org/10.1038/nrrheum.2012.64>.
 67. Allison AC. 2000. Immunosuppressive drugs: the first 50 years and a glance forward. *Immunopharmacology* 47:63–83. [http://dx.doi.org/10.1016/S0162-3109\(00\)00186-7](http://dx.doi.org/10.1016/S0162-3109(00)00186-7).